5
Quantum Description of Raman Scattering

The classical description of the Raman effect developed in Chapter 4 provides an account of the frequencies observed in the Raman spectra for carbon nanotubes, including quantitative descriptions of some of the main spectral features. The observed Raman lines are shifted in energy from the laser line in accordance with their phonon energies, with energy conservation occurring for each scattering process. For a quantitative description of the Raman intensities, a quantum description of the scattering processes is needed. In the case of sp^2 nanocarbons, a quantum treatment is essential because of the resonance Raman scattering process. Even for the main spectral features, their observed Raman frequencies depend strongly on the quantum description of the internal scattering events. The goal of this chapter is to introduce a quantum description of the Raman scattering process, starting with the Fermi Golden Rule, which provides a theoretical basis for the scattering process, ending with the form of the electron–photon and electron–phonon interaction Hamiltonians.

5.1
The Fermi Golden Rule

In this section we review a few of the results of time-dependent perturbation theory and the use of the Fermi Golden Rule to provide the background for a quantum mechanical description of the Raman effect in Section 5.2. A detailed discussion of these topics can be found in standard quantum mechanics text books [92, 200], since the development of the formalism of Raman spectroscopy depends strongly on the use of time-dependent electromagnetic fields. The most important case of interest is the one where the external field is a sinusoidal function of time. For most practical applications, the external fields are sufficiently weak, so that their effect can be handled within the framework of perturbation theory, where the unperturbed wavefunctions serve as a basis for describing the perturbed system. If the perturbation has an explicit time dependence, it must be handled by *time-dependent* perturbation theory.

Raman Spectroscopy in Graphene Related Systems. Ado Jorio, Riichiro Saito, Gene Dresselhaus, and Mildred S. Dresselhaus

ISBN: 978-3-527-40811-5

In doing time-dependent perturbation theory, we solve the time-dependent form of the Schrödinger equation, which is:

$$i\hbar\frac{\partial\psi}{\partial t} = \mathcal{H}\psi = (\mathcal{H}_0 + \mathcal{H}'(t))\psi \ , \tag{5.1}$$

where $\mathcal{H}'(t)$ is a time-dependent perturbation. We then expand the time-dependent wavefunctions $\psi(\boldsymbol{r}, t)$ in terms of the complete set of eigenfunctions of $\mathcal{H}_0$ $u_n(\boldsymbol{r})e^{-iE_nt/\hbar}$,

$$\psi(\boldsymbol{r}, t) = \sum_n a_n(t)u_n(\boldsymbol{r})\ e^{-iE_nt/\hbar} \ , \tag{5.2}$$

where the $a_n(t)$ are the time-dependent expansion coefficients. Combining Eq. (5.1) and Eq. (5.2) we obtain a relation

$$\dot{a}_m(t) = \frac{1}{i\hbar}\sum_n a_n(t)e^{i\omega_{mn}t}\langle m|\mathcal{H}'(t)|n\rangle \ , \tag{5.3}$$

where ω_{mn} is the Bohr frequency proportional to the energy difference between states m and n

$$\omega_{mn} = (E_m - E_n)/\hbar \ , \tag{5.4}$$

and $\langle m|\mathcal{H}'(t)|n\rangle$ is the time-dependent matrix element given by

$$\langle m|\mathcal{H}'(t)|n\rangle = \int u_m^*(\boldsymbol{r})\mathcal{H}'(t)u_n(\boldsymbol{r})d^3r \ . \tag{5.5}$$

Since $\mathcal{H}'(t)$ is time-dependent, so too are its matrix elements time-dependent.

In applying perturbation theory, we consider the matrix element $\langle m|\mathcal{H}'(t)|n\rangle$ to be small, and we write each time-dependent amplitude as an expansion in perturbation theory

$$a_m = a_m^{(0)} + a_m^{(1)} + a_m^{(2)} + \cdots = \sum_{i=0}^{\infty} a_m^{(i)} \ , \tag{5.6}$$

where the superscript (i) gives the order of each term in perturbation theory. Thus $a_n^{(0)}$ is the zeroth-order term and $a_n^{(i)}$ is the ith order correction to a_n. From Eq. (5.3), we see that $a_m(t)$ changes its value with time only because of the time-dependent perturbation. Thus, the unperturbed situation (zeroth-order perturbation theory) must give no time dependence in zeroth-order and has a value only for the initial state labeled ℓ

$$\dot{a}_m^{(0)} = 0, \quad \text{and} \quad a_m^{(0)} = \delta_{m\ell} \ , \tag{5.7}$$

where $\delta_{m\ell} = 1$ for $m = \ell$ and $\delta_{m\ell} = 0$ for $m \neq \ell$ (Kronecker's delta function). Then the first-order correction becomes:

$$\dot{a}_m^{(1)} = \frac{1}{i\hbar}\sum_n a_n^{(0)}\langle m|\mathcal{H}'(t)|n\rangle e^{i\omega_{mn}t} = \frac{1}{i\hbar}a_\ell^{(0)}\langle m|\mathcal{H}'|\ell\rangle e^{i\omega_{m\ell}t} \ . \tag{5.8}$$

For our interest here, if the perturbation $\mathcal{H}'(t)$ has a sinusoidal time dependence with frequency ω, which is the situation for all resonant phenomena, we can write

$$\mathcal{H}'(t) = \mathcal{H}'(0)e^{\pm i\omega t} . \tag{5.9}$$

This shows the explicit time dependence, so that upon integration of Eq. (5.8), and after some manipulation of terms, we obtain the probability for finding an electron in the state m, that is

$$|a_m^{(1)}(t)|^2 = \frac{|\langle m|\mathcal{H}'|\ell\rangle|^2}{\hbar^2} \frac{4\sin^2((\omega_{m\ell} \pm \omega)t/2)}{(\omega_{m\ell} \pm \omega)^2}, \quad (m \neq \ell) , \tag{5.10}$$

where ω is the applied frequency and $\omega_{m\ell}$ is the resonant frequency for the transition. Here the explicit time dependence is contained in an oscillatory term of the form $[\sin^2(\omega' t/2)/\omega'^2]$ where $\omega' = \omega_{m\ell} \pm \omega$. This function is also encountered in diffraction theory and looks like that shown in Figure 5.1.

Of special interest here is the fact that the main contribution to this function comes from $\omega' \cong 0$, with the height of the main peak proportional to $t^2/4$ and the width proportional to $1/t$. This means that the area under the central peak is proportional to $t/4$. If ω' becomes zero, the system makes a selective transition from a state ℓ to the corresponding state m with a transition probability proportional to t. If we then wait long enough, a system in an energy state ℓ will eventually make a transition to a state m, if photons of the resonant frequency $\omega_{\ell m}$ are present.[1)]

Since the transition probability is proportional to t, it is therefore useful to introduce the quantity called the *transition probability per unit time* and the relation giving this quantity is called Fermi's Golden Rule (named for Enrico Fermi who first introduced this rule to calculate such transition probabilities).

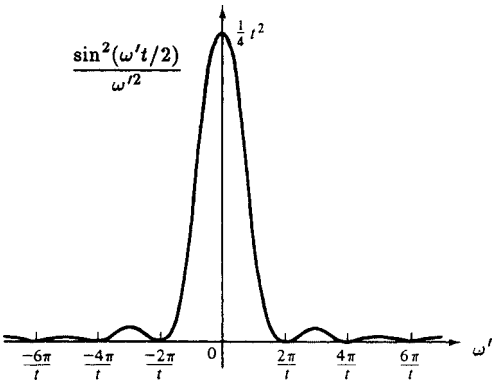

Figure 5.1 Plot of $\sin^2(\omega' t/2)/\omega'^2$ vs. ω', a function which enters the calculation of typical time-dependent perturbation problems [200].

1) When $|a_m^{(1)}|^2 \sim 1$, perturbation treatment can no longer be used. The increase of $|a_m^{(1)}|^2$ discussed here is valid when $|a_m^{(1)}|^2 \ll 1$.

In deriving Fermi's Golden Rule, we must consider the system to be exposed to the perturbation for a time sufficiently long, so that we can make a meaningful measurement within the framework of the Heisenberg uncertainty principle:

$$\Delta E \Delta t \sim \hbar \,, \tag{5.11}$$

so that the uncertainty in energy (or frequency) during the time that the perturbation acts is

$$\Delta E \sim h/t \tag{5.12}$$

or

$$\Delta \omega_{\ell m} \sim 2\pi/t \,. \tag{5.13}$$

But this is precisely the period of the oscillatory function shown in Figure 5.1. In this context, we must think of the concept of the transition probability/unit time as encompassing a range of energies and times consistent with the uncertainty principle. In the case of solids, it is quite natural to do this in any case, because the wave vector $\boldsymbol{k}$ is a quasi-continuous variable. That is, there are a large number of k states which have energies close to a given energy since the quantum states labeled by wave vector $\boldsymbol{k}$ are close together in a solid having about 10^{22} atoms/cm^3. Since the photon source itself has a bandwidth, we would automatically want to consider a range of energy differences $\hbar \delta \omega'$. From this point of view, we introduce the transition probability/unit time W_m for making a transition to a state m

$$W_m = \frac{1}{t} \sum_{m' \approx m} | \, a^{(1)}_{m'}(t) \, |^2 \,, \tag{5.14}$$

where the summation is carried out over a range of energy states consistent with the uncertainty principle; $\Delta \omega_{mm'} \sim 2\pi/t$.

Substituting for $|a^{(1)}_{m'}(t)|^2$ from Eq. (5.10), we obtain

$$|a^{(1)}_{m}(t)|^2 = \frac{4|\langle m|\mathcal{H}'|\ell\rangle|^2}{\hbar^2} \frac{\sin^2(\omega' t/2)}{\omega'^2} \tag{5.15}$$

and the summation in Eq. (5.16) is replaced by an integration over a narrow energy range weighted by the density of states $\rho(E_m)$ which denotes the number of states per unit energy range. We thus obtain

$$W_m = \frac{4}{\hbar^2 t} \int |\mathcal{H}'_{m'\ell}|^2 \frac{\sin^2(\omega_{m'\ell} t/2)}{\omega^2_{m'\ell}} \rho(E_{m'}) \, d E_{m'} \tag{5.16}$$

where we have written $\mathcal{H}'_{m'\ell}$ for the matrix element $\langle m'|\mathcal{H}'|\ell\rangle$. But, by hypothesis, we are only considering energies within a small energy range $E_{m'}$ around E_m and over this energy range the matrix elements and density of final states will not be varying much. However, the function $[\sin^2(\omega' t/2)/\omega'^2]$ will be varying rapidly, as can be seen from Figure 5.1. Therefore, it is adequate to integrate Eq. (5.16) only

over the rapidly varying function $[\sin^2(\omega t/2)]/\omega^2$. Writing $dE = \hbar d\omega'$, we then obtain

$$W_m \simeq \frac{4|\mathcal{H}'_{m\ell}|^2 \rho(E_m)}{t\hbar^2} \int \frac{\sin^2 \frac{\omega' t}{2}}{\omega'^2} d\omega' \,. \tag{5.17}$$

The most important contribution to the integral in Eq. (5.17) comes from values of ω close to ω'. On the other hand, we know how to do this integral between $-\infty$ and $+\infty$, since

$$\int_{-\infty}^{\infty} \frac{\sin^2 x}{x^2} dx = \pi \,. \tag{5.18}$$

Therefore we can write an approximate relation based on Eq. (5.17) by setting $x = \omega' t/2$

$$W_m \cong \frac{2\pi}{\hbar} |\mathcal{H}'_{m\ell}|^2 \rho(E_m) \,. \tag{5.19}$$

The simple formula in Eq. (5.19) is called Fermi's Golden Rule, and is used to calculate transition probabilities per unit time when considering the optical properties of solids, including Raman scattering intensities.

If the initial state is a discrete level (such as a donor impurity level) and the final state is a continuum (such as the conduction band), then the Fermi's Golden Rule (Eq. (5.19)), as written, yields the transition probability per unit time and $\rho(E_m)$ is interpreted as the density of *final* states. Likewise if the final state is discrete and the initial state is a continuum, then W_m also gives the transition probability per unit time, only in this case $\rho(E_m)$ is now interpreted as the density of initial states. If the transitions of interest are between a continuum of initial states and a continuum of final states, then the Fermi Golden Rule must be interpreted in terms of a joint density of states, whereby the initial and final states are separated by the photon energy $\hbar\omega$ inducing the transition.

Our discussion up to this point introduces the basic concepts behind Fermi's Golden Rule, that is it provides an understanding of each term in W_m and its relation to the uncertainty principle. For further interpreting Raman spectra, we need to consider first-order one-phonon scattering processes as well as second-order two-phonon scattering processes, as shown in Figures 5.2 and 5.3. Therefore, to describe the Raman processes we typically consider second-order and higher-order perturbation theory, where we start in an initial state, scatter into one or more intermediate states before scattering back to a final state. The expression for the Raman intensity obtained by these higher-order perturbation processes is given in Section 5.2. We do not derive the second-order and higher-order perturbation theory in this book since it is laborious, it does not add new physical insights and such derivations can be found in standard quantum mechanics texts [92, 200, 201]. In short, by increasing the order in perturbation theory, one matrix element and one more term in the denominator will be added, with a summation over all possible intermediate states, as described in the next section.

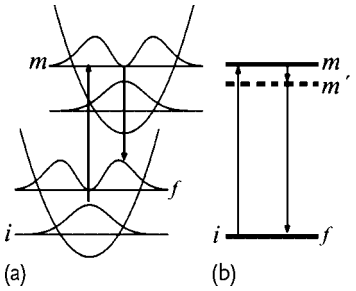

Figure 5.2 (a) Schematics showing the second-order Raman process for small molecules, where both the electronic (parabola) and vibrational levels are displayed, comparable to Figure 3.2. Notice the horizontal displacement of the two parabolas, indicating that the two different electronic levels have different atomic positions. The upwards arrow indicates vibronic state transition $i \rightarrow m$ mediated by the photon absorption, and the downwards arrow indicates vibronic state transition $m \rightarrow f$ mediated by the photon emission. The energy difference between the incident and scattered photons corresponds to a quantum of atomic vibration. (b) Schematics showing the third-order process often used to describe the Raman process in crystals. While the large upwards $i \rightarrow m$ and downwards $m' \rightarrow i$ arrows represent photon absorption and emission by the electron, the small downwards arrow $m \rightarrow m'$ represents the electron losing energy to the lattice through an electron–phonon scattering event. The vibrational levels are not displayed.

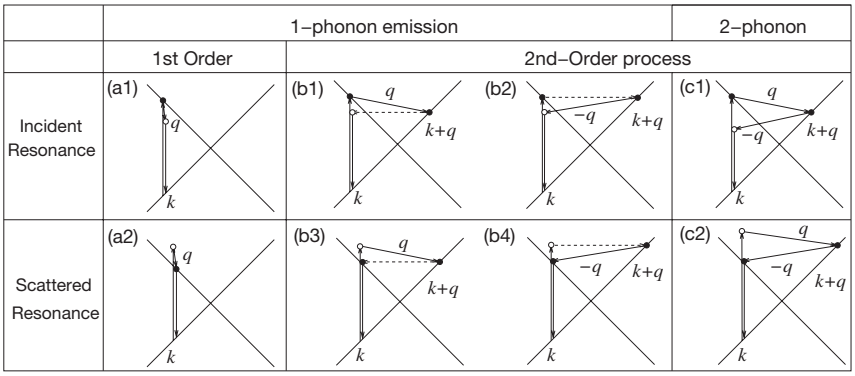

Figure 5.3 (a) One-phonon first-order, (b) one-phonon second-order, and (c) two-phonon second-order, resonance Raman spectral processes. Parts (a1), (b1), (b2), and (c1) show incident photon resonance conditions, and parts (a2), (b3), (b4), and (c2) show scattered photon resonance conditions. For one-phonon second-order transitions, one of the two scattering events is an elastic scattering event (dashed lines). Resonance points are shown as solid circles [80].

5.2 The Quantum Description of Raman Spectroscopy

In computing the Raman spectra related to totally symmetric phonons in small molecules, we make use of the Frank–Condon effect, whereby the excitation of one electron by a photon changes the atomic arrangement in a molecule, so that an

overlap between the vibrational states n_q and $n_q + 1$ is possible (see Figure 5.2a). That is, since the excited states have different wavefunctions which give a different stable position for the atom in the molecule, the atom in the excited state moves from its original position in the ground state, thereby inducing an atomic vibration. Each of the four levels displayed in Figure 5.2a represents a different *vibronic* level, which designates a given electronic and vibrational level.

In larger molecules or crystals, however, exciting one electronic state does not change the atomic configuration, and second-order perturbation theory can only give rise to elastic (Rayleigh) scattering of the light. In these cases, it is necessary to go to third-order perturbation theory, whereby the excited electron perturbs the atom in creating a phonon through an electron–phonon interaction. Such a process is sketched in Figure 5.2b and is different from Figure 5.2a, where both the electronic and vibrational levels are displayed, showing a transition between vibronic states. In Figure 5.2b only the electronic energies are displayed, and the system is described as having the same initial and final electronic level, although one phonon has been left in the system, mediated by the electron–phonon scattering event represented by the small downwards arrow. Figure 5.2b is pictorial, and the excited energy levels m and m' do not necessarily represent real electronic states, but just the energy gained by the electron from its original energy E_i, as discussed below.

If the electron is initially in a state i with energy E_i, then light scattering can excite the electron to a higher energy state m with energy E_m (see Figure 5.2b) by the absorption of an excitation energy $(E_m - E_i)$ from a laser (E_{laser}). If m is a real electronic state (we usually draw a solid line), the light absorption is a resonant process. This electron will be further scattered by a $q \approx 0$ phonon to a "virtual" state m', and decay back to state i by emitting the scattered light. Virtual states are usually displayed by dashed lines and, within perturbation theory, they are described by a linear combination of the electron eigenstates of the system with a large energy uncertainty and a small lifetime to compensate for the uncertainty principle. The initial "system", therefore, has an electron in the state i and a photon with energy $(E_m - E_i)$, while the final "system" has an electron in the state i, a phonon of energy E_q and a photon with energy $(E_m - E_i - E_q)$. Alternatively, the incident photon can excite the electron to a virtual state m with higher energy E_m and light scattering can serve to bring the system to a final state of lower energy E_i by the emission of energy $(E_m - E_i)$. In this case, it is the photon emission that is resonant, rather than the photon absorption. This alternative process is shown in Figure 5.3a2. While in Figure 5.2b we show discrete electronic levels, in Figure 5.3 we show Raman scattering processes within the continuum electronic dispersion near the Fermi level at the K point of graphene (see Section 2.2.2). Figure 5.3a1 is analogous to Figure 5.2b, and Figure 5.3a2 shows first-order Raman scattering with a resonant process involving the scattered light, while the other cases in Figure 5.3 show other possible processes discussed later.

Therefore, the first-order Raman intensity as a function of phonon energy $E_q = \hbar\omega_q$ and of the incident laser energy E_{laser} is given by third-order perturbation

theory by [91, 142]

$$I(\omega_q, E_{\text{laser}}) = \sum_f \left| \sum_{m,m'} \frac{M^{\text{op}}(\boldsymbol{k}-\boldsymbol{q}, i\,m') M^{\text{ep}}(\boldsymbol{q}, m'm) M^{\text{op}}(\boldsymbol{k}, mi)}{(E_{\text{laser}} - \Delta E_{mi})(E_{\text{laser}} - \hbar\omega_q - \Delta E_{m'i})} \right|^2 , \tag{5.20}$$

in which

$$\Delta E_{m^{(\prime)}i} \equiv (E_{m^{(\prime)}} - E_i) - i\gamma_r , \tag{5.21}$$

and i, m, m' and f denote, respectively, the initial state, the two excited intermediate states, and the final state of an electron, while γ_r denotes the broadening factor of the resonance event (see Section 4.3.2.5). The physical process is described by an electron at wave vector $\boldsymbol{k}$ that is (1) excited by an electric dipole interaction $M^{\text{op}}(\boldsymbol{k}, mi)$ with the incident photon to make a transition from state i to m, and the electron is then (2) scattered by emitting a phonon with energy $\hbar\omega_q$ and wave vector $\boldsymbol{q}$ through an electron–phonon interaction, $M^{\text{ep}}(\boldsymbol{q}, m'm)$, and finally (3) the electron in state m' emits a photon by an electric dipole transition, through the interaction $M^{\text{op}}(\boldsymbol{k}-\boldsymbol{q}, i\,m')$ to reach the final electronic state $f = i$. For momentum conservation, $q \approx 0$. For an energy separation E_{im} between the i and m states, the resonance conditions are either with the incident photon, $E_{\text{laser}} = E_{mi}$, or with the scattered photon, $E_{\text{laser}} = E_{mi} + \hbar\omega_q$. To reach a given final state, the sum in Eq. (5.20) is taken over all possible intermediate states m and m'. The intermediate states m are determined by specifying the initial state i with use of energy-momentum conservation. In order to take the sum over the intermediate states, we need to know the electric dipole matrix elements of the electron–photon interaction, M^{op}, and of the electron–phonon interaction, M^{ep}, which will be discussed in Section 5.4. In the scattering process, energy-momentum conservation for an electron and phonon holds, but this is not explicitly written in Eq. (5.20).

Moving to a higher-order Raman process, the various diagrams in Figure 5.3b1–b4 and 5.3c1,c2 show inelastic scattering processes which have to be described by fourth-order perturbation theory. In Figure 5.3b1–b4, there is an internal electron scattering process by a phonon, and another by a lattice defect or impurity, which can cause an elastic scattering event. Both phonon emission and absorption are possible and the order of the elastic and inelastic scattering processes can be interchanged. These processes will be discussed in Chapter 13. Figure 5.3c1,c2 shows two second-order two-phonon Raman scattering processes. In this case, the intensity as a function of E_{laser} and the sum of the two phonon energies $\omega = \omega_1 + \omega_2$ is given by a similar formula,

$$I(\omega, E_{\text{laser}}) \propto \sum_i \left| \sum_{m',m'',\omega_1,\omega_2} J_{m',m''}(\omega_1, \omega_2) \right|^2 , \tag{5.22}$$

where

$$J_{m',m''}(\omega_1, \omega_2) = \frac{M^{\text{op}}(\boldsymbol{k}, i\,m'') M^{\text{ep}}(-\boldsymbol{q}, m''m') M^{\text{ep}}(\boldsymbol{q}, m'm) M^{\text{op}}(\boldsymbol{k}, mi)}{(E_{\text{laser}} - \Delta E_{mi})(E_{\text{laser}} - \hbar\omega_1 - \Delta E_{m'i})(E_{\text{laser}} - \hbar\omega_1 - \hbar\omega_2 - \Delta E_{m''i})} . \tag{5.23}$$

Now we have two-phonon scattering processes with phonon wave vectors $\boldsymbol{q}$ and $-\boldsymbol{q}$, so that momentum conservation is possible with $q \neq 0$. Due to momentum conservation for the whole process, most often the m'' and m states will be the same, since all the others will generally be much farther in energy. In order to get two resonance conditions at the same time, an intermediate electronic state $E_{m'i}$ is always in resonance ($E_{\text{laser}} = \Delta E_{m'i} + \hbar\omega_1$), and either the incident resonance condition ($E_{\text{laser}} = \Delta E_{mi}$) or the scattered resonance condition ($E_{\text{laser}} = \Delta E_{m''i} + \hbar\omega_1 + \hbar\omega_2$) is satisfied. On the other hand, for a second-order one-phonon process, the Raman intensity is calculated by replacing one of the two phonon scattering processes by an elastic impurity scattering process. Another point to mention concerns the energy uncertainty γ_r, which enters Eq. (5.21) and is operative in Eqs. (5.20) and (5.23). Actually, the different denominators may have different γ_r values since they are related to different scattering events. However it is usual to consider the same γ_r for simplicity when there is no experimental information distinguishing them. The physical origin of γ_r has been discussed in Section 4.3.2.5.

5.3 Feynman Diagrams for Light Scattering

Feynman diagrams are useful for keeping track of various processes that may occur in an inelastic scattering process that absorbs or creates an excitation, such as the six scattering processes shown in Figure 5.4a–f for creating an excitation (e. g., the Raman Stokes process). The basic notation used in drawing Feynman diagrams consists of propagators, such as electrons, phonons or photons and vertices where interactions occur, as shown in Figure 5.4g. Time goes from left to right in the diagrams in Figure 5.4. The basic diagram for the Raman process is given in Figure 5.4a and is taken from the Yu and Cardona book "Fundamentals of Semiconductors" [202]. The other permutations of Figure 5.4a obtained by different orders of the vertices are given in Figure 5.4b–f and are also found in [202]. We then use the Fermi Golden Rule (Eq. (5.19)) for each diagram, by multiplying the contributions from each vertex. For example, the first vertex in Figure 5.4a contributes a term to the scattering probability per unit time of the form

$$\frac{\langle n|\mathcal{H}_{eR}(\omega_{\text{laser}})|i\rangle}{[E_{\text{laser}} - (E_n - E_i)]},$$

where the Hamiltonian $\mathcal{H}_{eR}(\omega_{\text{laser}})$ denotes the interaction between the electron and the incident electromagnetic radiation field ($\omega_i = \omega_{\text{laser}}$) taking the system from an initial state i to an intermediate state n. The interaction energy for the second vertex $\mathcal{H}_{\text{e-ion}}(\omega_{\text{laser}})$ is between the electron and the lattice vibrations of the ion (or the electron–phonon interaction) and the corresponding energy denominator is

$$E_{\text{laser}} - (E_n - E_i) - \hbar\omega_q - (E_{n'} - E_n) = [E_{\text{laser}} - \hbar\omega_q - (E_{n'} - E_i)] .$$

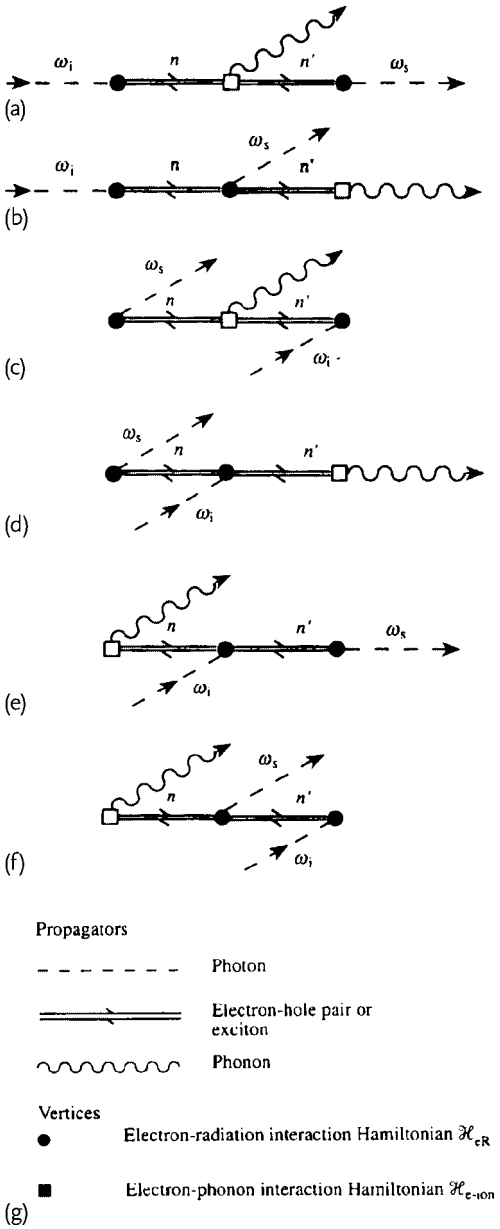

Figure 5.4 (a–f) Feynman diagrams for the six scattering processes that contribute to one-phonon (Stokes) Raman scattering. Here $\omega_i = \omega_{\text{laser}}$ and ω_s is the scattered light frequency. (g) Symbols used in drawing Feynman diagrams to represent Raman scattering [202].

Here $E_{\text{laser}} = \hbar\omega_{\text{laser}}$, $\hbar\omega_q$ is the phonon energy, E_i is the electron energy in the initial state and $E_{n(')}$ is the electron energy in the intermediate state. For the third vertex the denominator becomes $[E_{\text{laser}} - \hbar\omega_q - \hbar\omega_s - (E_f - E_i)]$, but since the initial and final electron energies are the same, energy conservation requires the δ function $\delta(\hbar\omega_{\text{laser}} - \hbar\omega_q - \hbar\omega_s)$ to yield the probability per unit time for Raman scattering for the diagram in Figure 5.4a:

$$P_{\text{ph}}(\omega_s) = \frac{2\pi}{\hbar}\left|\sum_{n,n'}\frac{\langle i|\mathcal{H}_{eR}(\omega_s)|n'\rangle\langle n'|\mathcal{H}_{\text{e-ion}}|n\rangle\langle n|\mathcal{H}_{eR}(\omega_{\text{laser}})|i\rangle}{[E_{\text{laser}} - (E_n - E_i)][E_{\text{laser}} - \hbar\omega_q - (E_{n'} - E_i)]}\right|^2 \times \delta(E_{\text{laser}} - \hbar\omega_q - \hbar\omega_s)\,, \tag{5.24}$$

in which $\hbar\omega_s$ denotes the photon energy for the scattered light.

The rules in drawing Feynman diagrams are:

- Excitations such as photon, phonons and electron–hole pairs that occur in Raman scattering are represented by lines (or propagators). These propagators can be labeled by the properties of the excitations, such as their wave vectors, frequencies and polarizations.
- The interaction between two excitations is represented by an intersection of their propagators. This intersection is known as a *vertex* and is sometimes highlighted by a symbol such as a filled circle (electron–photon interaction) or an empty square (electron–phonon interaction).
- Propagators are drawn with an arrow to indicate whether excitations are created or annihilated in an interaction. Arrows pointing towards a vertex represent excitations which are annihilated. Those pointing away from the vertex are for excitations that are created.
- When several interactions are involved, they are always assumed to proceed sequentially from the left to the right as a function of time.
- Once a diagram has been drawn for a certain process, other possible processes are derived by permuting the time order in which the vertices occur in the Feynman diagram.

Then summing over the six diagrams in Figure 5.4 yields the result

$$\begin{aligned}P_{\text{ph}}(\omega_s) = \frac{2\pi}{\hbar}\Bigg|\sum_{n,n'}&\frac{\langle i|\mathcal{H}_{eR}(\omega_s)|n'\rangle\langle n'|\mathcal{H}_{\text{e-ion}}|n\rangle\langle n|\mathcal{H}_{eR}(\omega_{\text{laser}})|i\rangle}{[\hbar\omega_i - (E_n - E_i)][\hbar\omega_i - \hbar\omega_q - (E_{n'} - E_i)]}\\ &+\frac{\langle i|\mathcal{H}_{\text{e-ion}}|n'\rangle\langle n'|\mathcal{H}_{eR}(\omega_s)|n\rangle\langle n|\mathcal{H}_{eR}(\omega_{\text{laser}})|i\rangle}{[\hbar\omega_i - (E_n - E_i)][\hbar\omega_i - \hbar\omega_s - (E_{n'} - E_i)]}\\ &+\frac{\langle i|\mathcal{H}_{eR}(\omega_{\text{laser}})|n'\rangle\langle n'|\mathcal{H}_{\text{e-ion}}|n\rangle\langle n|\mathcal{H}_{eR}(\omega_s)|i\rangle}{[-\hbar\omega_s - (E_n - E_i)][-\hbar\omega_s - \hbar\omega_q - (E_{n'} - E_i)]}\\ &+\frac{\langle i|\mathcal{H}_{\text{e-ion}}|n'\rangle\langle n'|\mathcal{H}_{eR}(\omega_{\text{laser}})|n\rangle\langle n|\mathcal{H}_{eR}(\omega_s)|i\rangle}{[-\hbar\omega_s - (E_n - E_i)][-\hbar\omega_s + \hbar\omega_i - (E_{n'} - E_i)]}\end{aligned}$$

$$+\frac{\langle i|\mathcal{H}_{eR}(\omega_s)|n'\rangle\langle n'|\mathcal{H}_{eR}(\omega_{\text{laser}})|n\rangle\langle n|\mathcal{H}_{\text{e-ion}}|i\rangle}{[-\hbar\omega_q-(E_n-E_i)][-\hbar\omega_q+\hbar\omega_i-(E_{n'}-E_i)]}$$
$$+\frac{\langle i|\mathcal{H}_{eR}(\omega_{\text{laser}})|n'\rangle\langle n'|\mathcal{H}_{eR}(\omega_s)|n\rangle\langle n|\mathcal{H}_{\text{e-ion}}|i\rangle}{[-\hbar\omega_q-(E_n-E_i)][-\hbar\omega_q-\hbar\omega_s-(E_{n'}-E_i)]}\Bigg|^2$$
$$\times\,\delta(\hbar\omega_i-\hbar\omega_s-\hbar\omega_q)\,. \tag{5.25}$$

Here we used $\hbar\omega_i$ instead of E_{laser}. Notice that having $\hbar\omega_i$ in the denominators or not depends on the position (time ordering) at which the optical absorption takes place in the Feynman diagram, and not all terms can be resonant, that is, when one of the terms in the denominator vanishes, the transition probability diverges and a resonance process takes place. Therefore, while all the terms in Eq. (5.25) play a role in nonresonant Raman scattering, when considering resonance Raman scattering with a fixed energy between the valence and conduction bands, only one of the terms in Eq. (5.25) will dominate. Interestingly, this is exactly the term where scattering occurs in the most intuitive order of events, that is, light absorption, electron–phonon scattering, light emission (first term in Eq. (5.25)). For this reason, the simpler Eq. (5.20) is enough for the calculation of Raman intensities under resonance conditions. This concept is developed further in the problem set for this chapter.

5.4 Interaction Hamiltonians

In this section we discuss the form of the interaction Hamiltonian $\mathcal{H}_{eR}$, which denotes the interaction between the electron and the electromagnetic radiation field (the electron–photon interaction), and the interaction Hamiltonian $\mathcal{H}_{\text{e-ion}}$ is between the electron and the lattice vibrations of the ion (or the electron–phonon interaction). Together with information about the electronic and vibrational states, plus the exciting field, these Hamiltonians can be used to calculate the matrix elements M^{op} and M^{ep}.

5.4.1 Electron–Radiation Interaction

The Hamiltonian $\mathcal{H}_{eR}$ that can be used to obtain the Lorentz force for an electron in an electromagnetic field is given by:

$$\mathcal{H}_{eR}=\frac{1}{2m}(\boldsymbol{p}-e\boldsymbol{A})^2+V(\boldsymbol{r})\,, \tag{5.26}$$

where m and e are the electron mass and charge, $\boldsymbol{p}$, $\boldsymbol{A}$ and $V(\boldsymbol{r})$ are, respectively, the momentum, vector potential and crystal potential. This is known from classical electromagnetism theory, that in the presence of an electromagnetic field,

the canonical momentum has to be substituted by $\boldsymbol{p} \rightarrow \boldsymbol{p} - e\boldsymbol{A}$ written here in S.I. units. In the Coulomb gauge ($\nabla \cdot \boldsymbol{A} = 0$), then $\boldsymbol{p}$ and $\boldsymbol{A}$ commute and Eq. (5.26) becomes

$$\mathcal{H}_{eR} = \left[\frac{\boldsymbol{p}^2}{2m} + V(\boldsymbol{r})\right] - \frac{e}{m}\boldsymbol{p}\cdot\boldsymbol{A} + \frac{e^2\boldsymbol{A}^2}{2m} \,. \tag{5.27}$$

The term between brackets gives the Hamiltonian $\mathcal{H}_0$ for an electron in the potential $V(\boldsymbol{r})$. Considering electromagnetic fields that are not so intense, the $\boldsymbol{A}^2$ term can be neglected (weak field approximation), and the electron-electromagnetic field interaction is given by:

$$\mathcal{H}_{eR} = -\frac{e}{m}\boldsymbol{p}\cdot\boldsymbol{A} \,. \tag{5.28}$$

For light scattering by a crystal, the wavelength of light is much larger than the unit cell dimensions, and an electron basis wavefunction $\varphi(\boldsymbol{r})$ (for example, a tight-binding wavefunction) is localized around the position of an atom $\boldsymbol{r}_0$ (a situation that is also valid for light scattering by a molecule). Considering monochromatic plane waves ($\boldsymbol{A}(\boldsymbol{r}, t) \propto e^{i\boldsymbol{k}\cdot\boldsymbol{r}}$), the interaction Hamiltonian $\mathcal{H}_{eR}$ can be considered within the dipole approximation, which is represented by $\boldsymbol{A}(\boldsymbol{r}, t)|\Psi\rangle \approx \boldsymbol{A}(\boldsymbol{r}_0, t)|\Psi\rangle$.

Finally, by considering $\boldsymbol{p} \equiv m(d\boldsymbol{r}/dt)$, we can write $\mathcal{H}_{eR}$ in terms of the electric field and the position vector by

$$\mathcal{H}_{eR} = -e\boldsymbol{r}\cdot\boldsymbol{E}(\boldsymbol{r}_0, t) \,. \tag{5.29}$$

A third approximation has been considered, that is, the contribution from the derivative $\partial[\boldsymbol{r}\cdot\boldsymbol{A}(\boldsymbol{r}_0, t)]/\partial t$ vanishes, considering the time average over a complete field oscillation period.

5.4.2
Electron–Phonon Interaction

The Hamiltonian $\mathcal{H}_{\text{e-ion}}$ for the electron–phonon interaction describes how the energy of the atoms change when they move through the so-called deformation potential [203]

$$\mathcal{H}^{\sigma}_{\text{e-ion}}(\boldsymbol{R}_{S'}, \boldsymbol{R}_S) = \int \phi(\boldsymbol{r} - \boldsymbol{R}_{S'})\nabla v(\boldsymbol{r} - \boldsymbol{R}_\sigma)\phi(\boldsymbol{r} - \boldsymbol{R}_S)d^3r \,, \tag{5.30}$$

where $\phi(\boldsymbol{r} - \boldsymbol{R}_S)$ is the electron wave function at site $\boldsymbol{R}_S$ and $v(\boldsymbol{r} - \boldsymbol{R}_\sigma)$ is the atomic potential.[2)] Calculation of the electron–phonon interaction in nanocarbons will be treated in Section 11.7, but considering here a simplified picture, the electron–phonon matrix element for optical phonons can be obtained from the shift of the

2) For completeness, when calculating these matrix elements for determining the electron–phonon coupling, both electrons and holes have to be taken into account.

electronic bands under the deformation of the atomic structure corresponding to the phonon-pattern by [204, 205]

$$M^{\mathrm{ep}}(\boldsymbol{k}-\boldsymbol{q}, mm') = \sqrt{\frac{\hbar}{2N_\Omega M\omega_q}} \sum_a \varepsilon_a^q \frac{\partial E_m}{\partial u_a} \,, \tag{5.31}$$

where the sum over a runs over all atoms in the unit cell. The wave vector and band index of the electronic state are here denoted by k and m, respectively. The q index denotes the phonon with polarization vector ε_a^q while E_m is the electronic energy and u_a is the atomic displacement. N_Ω, M and ω_q are the number of unit cells in the system, the atomic mass and the phonon eigenvalue, respectively.

5.5
Absolute Raman Intensity and the E_{laser} Dependence

In Eqs. (5.20) and (5.22) the Raman intensity is given as proportional to the transition probability. Different authors present different proportionality constants, and measuring the absolute Raman intensity is not an easy task, since it depends on several experimental details. The simplest procedure is calibrating the Raman intensities experimentally by measuring the Raman spectra of a well-established Raman scatterer, such as a standard reference material. For example, the dependence of the absolute Raman cross-sections for the cyclohexane liquid (C_6H_{12}) are known from the literature [206].

Of special interest in this proportionality constant is a ω_s^4-dependence predicted by Raman scattering theory [207–215]. This ω_s^4 dependence is not a special result of Raman spectroscopy, but it comes from the general theory for dipole radiation [216]. In short, let's define the dipole moment by $\boldsymbol{d} = e\boldsymbol{r}$, where e is the electric charge and $\boldsymbol{r}$ is the vector connecting the negative and positive charges in the dipole. It is known that radiation occurs only when the electric charge exhibits acceleration. For this reason, the fields (H and E) are proportional to the second time-derivative of the dipole momentum, that is H and $E \propto \ddot{\boldsymbol{d}} = e\ddot{\boldsymbol{r}}$ describing $\boldsymbol{r} = \boldsymbol{r}_0 e^{i\omega_s t}$, $\ddot{\boldsymbol{d}} = -\omega_s^2 \boldsymbol{d}$. In addition, the scattering intensity I can be related to the energy flux given by the Poynting vector S which, for plane waves, is related to the squared fields ($I \propto S \propto H^2$ or $E^2 \propto (\ddot{\boldsymbol{d}})^2$). This gives rise to a ω_s^4 dependence for the light emission.[3)] It is true that in Raman spectroscopy the incident and scattered light have different energies from one another but, since the phonon energies involving $\hbar\omega_q$ are usually much smaller than the excitation laser energy, $\hbar\omega_i \sim \hbar\omega_s$ is a good approximation and we can thus say that the absolute Raman intensity should increase with E_{laser}^4.

3) This is also the reason why the sky is blue. For more details, see [216].

Problems

[5-1] Using Maxwell's equations, explain why we need a gauge field for the vector potential **A** and a static potential ϕ. Consider some gauges explicitly and explain under what kind of situation such gauges are useful by giving some explanation of the physical phenomena.

[5-2] In a vacuum, show that the electric field is expressed by the vector potential **A**.

[5-3] When we consider the Hamiltonian in the presence of a vector potential, expand the Hamiltonian and retain the linear term in **A**. This corresponds to a perturbation Hamiltonian for the electron–photon coupling constant. Use the Coulomb gauge $\mathrm{div}\,\mathbf{A} = 0$ when you obtain this result.

[5-4] In the previous problem, we also have a term which is proportional to $\mathbf{A}^2$. In order to neglect this term, this term should be at least 1/10 smaller than the linear **A** term. What is the corresponding value of the electric field? If **A** gives an electric field above this value, we should then consider the nonlinear $\mathbf{A}^2$ effect of light.[4)]

[5-5] The Poynting vector, $\mathbf{S} = \mathbf{E} \times \mathbf{H}$ is the power density per unit area of the electromagnetic field. In a typical micro-Raman measurement system, the diameter of the light beam is about 1 μm and the laser power is 1 mW. Estimate the power density of this micro-Raman setup and calculate **E**. Show that the electric field thus obtained is not strong enough to be in the nonlinear regime.

[5-6] Show that there is C_2 rotational symmetry in graphene. C_2 rotational symmetry means that the lattice structure does not change under a 180° rotation about a point. Specify the symmetry axis of this C_2 rotation.

[5-7] By the C_2 rotation, the A and B carbon atoms in the unit cell are exchanged with each other. Show that all A and B carbon atoms in the lattice are exchanged for any C_2 rotation.

[5-8] When we put the origin of the coordinate system at the axis point of the C_2 rotation of graphene, show that the perturbation Hamiltonian for the interaction of graphene with an incident light beam is an odd function of the coordinates.

[5-9] When we solve a simple 2×2 tight-binding Hamiltonian for the π-band of graphene (Eq. (2.29)), we get the wavefunction $\Psi(\boldsymbol{k})$ as a linear combination of the Bloch functions $\Phi_A(\boldsymbol{k})$ and $\Phi_B(\boldsymbol{k})$ consisting of A and B terms:

$$\Psi(\boldsymbol{k}) = C_A(\boldsymbol{k})\Phi_A(\boldsymbol{k}) + C_B(\boldsymbol{k})\Phi_B(\boldsymbol{k}) \,.$$

4) The general nonlinear optical effect in materials occurs at a much lower power level for light since the physical properties are saturated as a function of E. For example, the polarization vector **P** can be expanded as $\alpha E + \alpha^{(2)} E^2 + \ldots$, etc.

Obtain the explicit form of $C_A(\boldsymbol{k})$ and $C_B(\boldsymbol{k})$ for $s = 0$ in Eq. (2.29) with the use of $f(k)$ and $w(k)$ as defined in Eqs. (2.28) and (2.31), respectively.

[5-10] In the calculation for Problem 5-9, show $C_A = C_B$ and $C_A = -C_B$ for the valence and conduction band, respectively, for any $\boldsymbol{k}$ point. Combining this result with the fact that the perturbation Hamiltonian is an odd function of the coordinates for exchanging A and B, obtain the dipole transition matrix element which is proportional to $\langle \pi^* | \nabla | \pi \rangle$ as a function of $\boldsymbol{k}$.

[5-11] Using time-dependent perturbation theory, obtain the result for $|a_m^{(1)}(t)|^2$ in Eq. (5.10).

[5-12] Plot $|a_m^{(1)}(t)|^2$ in Eq. (5.10) for the case of $\omega_{m\ell} = \omega/2$, $2\omega/3$, $3\omega/4$, and ω. Show that the peak height of the oscillation is increasing as $\omega_{m\ell}$ increases. This means that we can select only the closest m states for the calculation of $|a^{(1)}(t)|^2$ as a first approximation.

[5-13] A delta function $\delta(x)$ has two significant properties: (1) The values of $\delta(x) = \infty$ for $x = 0$, but $= 0$ for $x \neq 0$. (2) When we integrate $\delta(x)$ over any region which includes $x = 0$, the integrated value is 1. Using these definitions, obtain the following formula:

$$\lim_{t \to \infty} \frac{\sin^2(\alpha t)}{\pi \alpha^2 t} = \delta(\alpha) \,,$$

and then, using this formula, obtain Fermi's Golden Rule directly.

[5-14] The uncertainty relation of $\Delta E \Delta t \sim \hbar$ (Eq. (5.11)) is important in spectroscopy since most optical processes have a finite lifetime. If an excited state has a lifetime Δt, the energy of the excited states has an energy uncertainty value ΔE. In this case, time-dependent theory in which we consider a definite energy, should be modified. Explain how the resonance condition can be relaxed in the case of such a lifetime.

[5-15] For a photoexcited electron in a carbon nanotube, the electron can emit a phonon within 1 ps. Estimate the uncertainty energy value for this electron. For the photoluminescence process for which a photon is emitted, the excited electron has a relatively slower lifetime, on the order of 1 ns. Is the accuracy of the spectrometer sufficient to observe the energy of a photoluminescent phonon?

[5-16] Analyze the first-order processes depicted in the Feynman diagrams of Figure 5.4 within the framework of a resonant process, which is obtained by having null terms in Eq. (5.25). By starting with a given $\hbar\omega_i$ and the material in the ground state, which processes can be and which cannot be resonant? Consider $n = n'$ for simplicity, which happens when the phonon does not break the symmetry of the system.

[5-17] In the previous problem, derive a quantitative analysis to understand which of the six processes in Eq. (5.25) dominate the total intensity. Choose values

for $E_m - E_i$ and for $\hbar\omega_q$ and introduce the damping term $i\gamma_r$ with a specific value for γ_r. You will realize that processes which seem "reasonable" within our own "common sense" are closely related to whether or not the resonance condition is achieved.

[5-18] When we consider one optical-absorption, one optical-emission, and one phonon-emission vertex, we can obtain six possible Feynman diagrams. How many Feynman diagrams are expected if we change one phonon-emission vertex into a two phonon-emission vertex? Illustrate using some diagrams where the process starts from the optical absorption.

[5-19] Demonstrate Eqs. (5.28) and (5.29) making clear where each approximation is introduced.

[5-20] Show that for a periodic motion of charged particles forming a dipole d, and c is the velocity of light, the intensity of radiation with frequency ω is given by:

$$I = \frac{4\omega^2}{3c^3}|d|^2 \,. \tag{5.32}$$